

# A Layerless Additive Manufacturing Process based on CNC Accumulation

Yong Chen\*, Chi Zhou, Jingyuan Lao  
Epstein Department of Industrial and Systems Engineering  
University of Southern California, Los Angeles, CA 90089

\*Corresponding author: [yongchen@usc.edu](mailto:yongchen@usc.edu), (213) 740-7829

## ABSTRACT

Most current additive manufacturing processes are layer-based, that is building a physical model layer-by-layer. By converting 3-dimensional geometry into 2-dimensional contours, the layer-based approach can dramatically simplify the process planning steps. However, there are also drawbacks associated with the layer-based approach such as inconsistent material properties between various directions. In a recent NSF workshop on additive manufacturing, it is suggested to investigate alternative non-layer based approaches. In this paper, we present an additive manufacturing process without planar layers. In the developed testbed, an additive tool based on a fiber optics cable and a UV-LED has been developed. By merging such tools inside a liquid resin tank, we demonstrate its capability of building various 2D and 3D structures. The technical challenges related to the development of such a process are discussed. Some potential applications including part repairing and building around inserts have also been demonstrated.

**KEYWORDS:** Additive manufacturing, 5-axis SFF, CNC accumulation, build around inserts.

## 1. INTRODUCTION

Most current additive manufacturing (AM) processes are layer-based. For example, a three-dimensional (3D) beam  $AB$  in a beam structure as shown in Figure 1.a is first sliced into a set of two-dimensional (2D) layers; a physical model can then be built by stacking all the layers (refer to Figure 1.b). A significant benefit of the layer-based approach is that, by converting 3D geometry into 2D contours, its process planning is dramatically simplified. However, there are also drawbacks associated with the layer-based approach. For example, beam  $AB$  will have different material property depending on its building orientation. In comparison, a more ideal approach is to add material along the beam direction as shown in Figure 1.c. Such a layerless AM process can improve the building speed as well as the material property of the built beams.

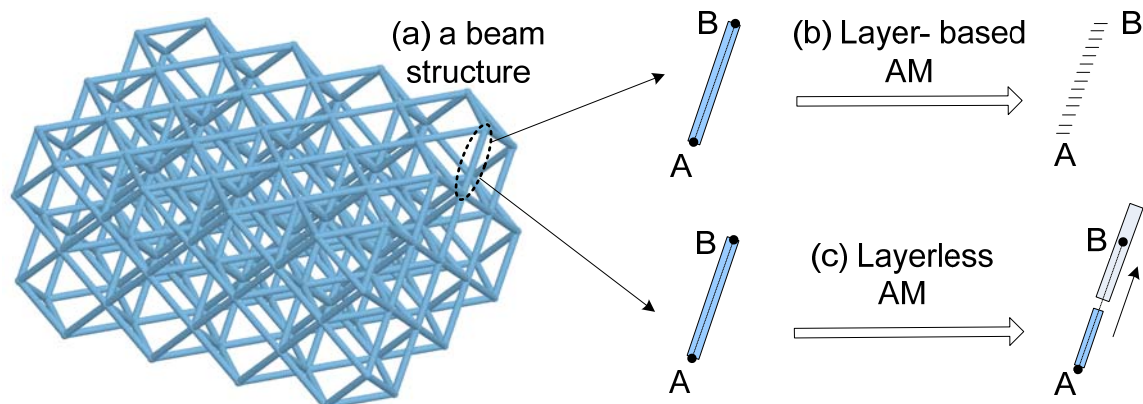


**Figure 1.** An illustration of the AM processes based on two different approaches.

Another drawback of the layer-based AM processes is the limitation on the allowable motions between the tools and the work pieces, which are mainly translational motions in  $X$ ,  $Y$ , and  $Z$  axes. Consequently, embedding existing components (i.e. building around inserts) in the processes is usually difficult. For example, Kataria and Rosen (2001) identified some major problems related to building

around inserts in the StereoLithography Apparatus (SLA) process including laser shadowing and vat recoating. Both of the problems are related to the layer-based approach.

Hence, developing non-layer-based methods has been identified as an important research direction for future AM development (Bourell, *et al.*, 2009). In this paper, we present a novel additive manufacturing process that is non-layer-based. The process is named Computer Numerically Controlled (CNC) accumulation due to its great similarity to the CNC machining process. As shown in Figure 2.a, the CNC machining process uses a machining tool to remove the material that is in touch with the tool. Hence, for a given work piece ( $W$ ) and tool path ( $S_i$ ) with tool orientation in each cutter location ( $O_j$ ), the constructed shape ( $M$ ) will be  $M = W - \cup(T)_{S_i+O_j}$ . In comparison, the CNC accumulation process as shown in Figure 2.b uses an accumulation tool to add material that is in touch with the tool. Hence, for tool path ( $S_i$ ) with tool orientation ( $O_j$ ), the constructed shape ( $M$ ) will be  $M = \cup(T)_{S_i+O_j}$ .

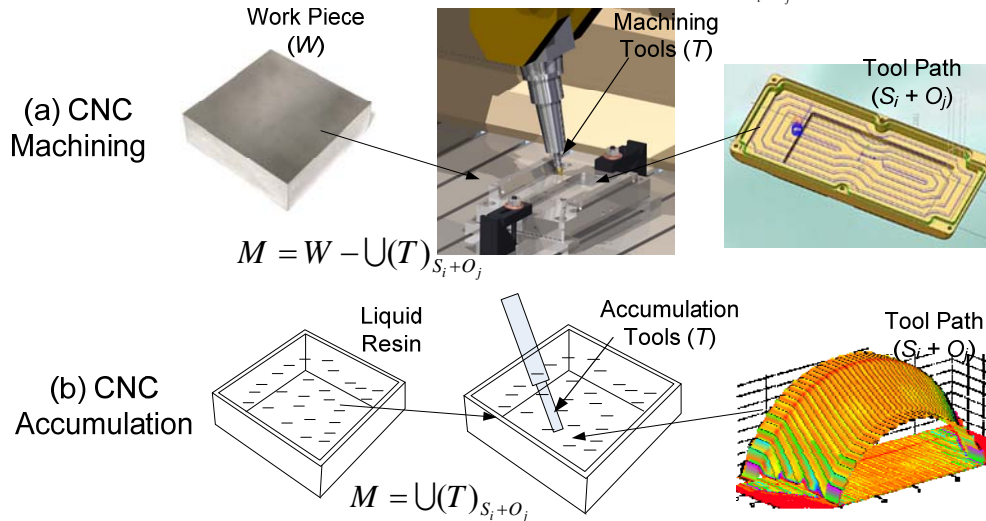


**Figure 2.** A comparison between CNC machining and CNC accumulation.

Both CNC machining and accumulation processes can have multi-axis tool motion. For example, various configurations of translations and rotations have been designed for 5-axis CNC machining systems such that much bigger allowable motions can be achieved between the machining tool and the work piece (Apró 2009). Recently the multi-axis CNC machining process has been increasingly popular due to its capability on improving part quality (e.g. surface finish) and reducing building time. Compared to the layer-based AM processes, one drawback associated with the multi-axis CNC machining and accumulation processes is that the tool path planning is more computationally challenging, since it requires to consider 3D instead of 2D problems. However, with the continuous improvement on high performance computing, significant advances in the multi-axis tool path planning have been and will continuously be made, which would dramatically mitigate such computational drawback.

## 2. PROCESS DESCRIPTION

We consider an additive manufacturing process based on UltraViolet(UV)-curable liquid resin such as the ones used in the SLA process. It is well known that a UV light source such as a laser can selectively cure liquid resin into solid parts. However, different from the SLA process, the curing tool in our process is merged under the liquid resin. Therefore, the accumulation tool is capable of curing resin in various directions. However, one main challenge related to allowing the curing tool to directly contact liquid resin is that a newly cured resin portion may attach to the curing tool instead of the base or the previously built part. We studied the attaching forces of such a portion that is constrained between the tip of the curing tool and the base or the previously built part (refer to Figure 3). The cured resin should attach to the base or the previously built part to ensure the building process to be successful. It was found this can be achieved if: (1) the attaching force between the cured resin and the tool can be reduced by applying certain types of coatings on the tool's tip; and (2) the attaching force between the cured resin

and the base or the previously built part can be sufficiently large by adjusting process parameters to ensure adequate over-curing. Our experimental setup is first presented as follows.

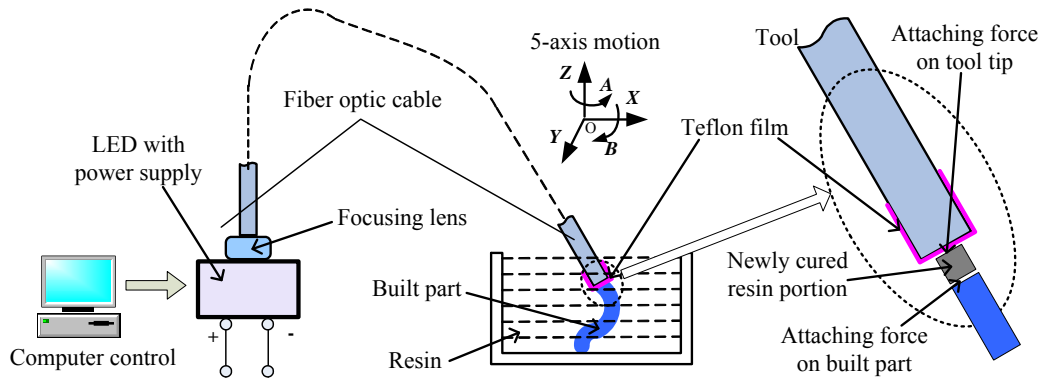


**Figure 3.** A schematic illustration of the CNC accumulation process.

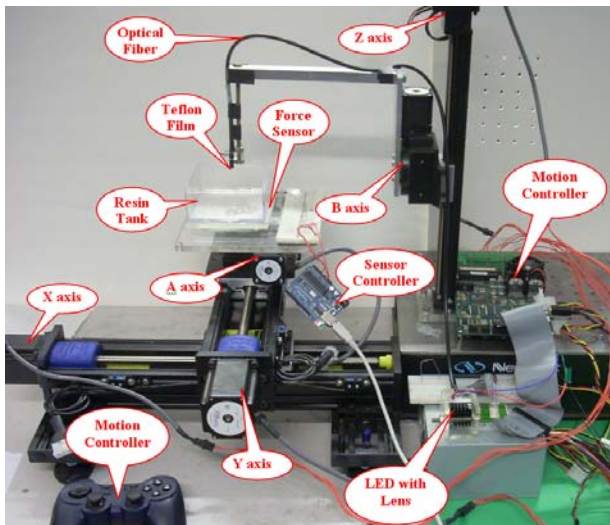


**Figure 4.** The hardware components of the CNC accumulation process.

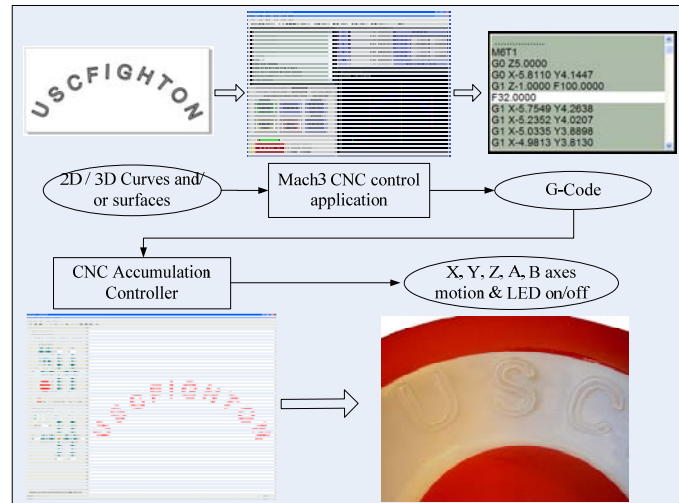


**Figure 5.** The software components of the CNC accumulation process.

## 2.1. Hardware Components

The hardware setup of our CNC accumulation system is shown in Figure 4. A high power UV-LED from *Nichia* (NCSU033A) is used as the curing light source. Compared to other technologies such as a UV-lamp and a UV-laser diode, a UV-LED has good properties such as inexpensive, low energy consumption, long lifetime and faster switching. On one side of the light guide, a sapphire ball lenses (NT43-831) and a quartz fiber optic light guide (NT38-954), both from *Edmunds Optics*, are used to focus and transmit UV light respectively. The other side of the light guide is merged in a resin tank as the curing tool. A 5-axis motion system that includes the  $X$ ,  $Y$ ,  $Z$  axes translation and  $A$ ,  $B$  axes rotation is designed to achieve controllable motion between the tool and the tank. The liquid resin used in our study is Accura Si60 from *3D Systems Inc.*

## 2.2. Software Components

The software setup of our CNC accumulation system is shown in Figure 5. For a given geometry, an off-the-shelf CNC machining software system, *Mach3* CNC control application ([www.machsupport.com](http://www.machsupport.com)), is used to convert a Computer-Aided Design (CAD) model into numeric control G-code. A developed CNC accumulation controller can read in the G-code and accordingly send commands to a motion controller to drive the 5 axis motion and to a micro-controller to control the LED state (i.e. ON/OFF). Hence a physical model can be built based on the planned tool path.

The remainder of the paper is organized as follows. Section 3 presents our study on the shape of the cured resin based on the developed tool. Section 4 and 5 present the attaching force models of the cured resin for point and line curing respectively. Section 6 presents the case studies on using the developed process to build various geometries. Section 7 presents two applications that illustrate the benefits of the developed process. Finally Section 8 concludes the paper.

### 3. CURING OF LIQUID RESIN

We first discuss the relation between the provided light energy and the related cured resin including its shape and size. Such understanding will provide the basis for the attaching force modeling as discussed in Sections 4 and 5.

#### 3.1. Principle

Jacobs (1992) studied the curing behavior of the SLA process based on a laser beam. For a given type of liquid resin, a critical energy exposure threshold ( $E_c$ ) can be found as the minimum energy requirement. According to the Beer-Lambert exponential law of absorption, the laser exposure will decrease exponentially with depth  $z$ . Based on the depth of penetration of resin ( $D_p$ ), the dependence of curing depth  $C_d$  upon the maximum exposure at the resin surface follows the equation:

$$C_d = D_p \ln(E_{\max} / E_c) \quad (3.1)$$

Also as shown in (Jacobs 1992), a cured line in the shape of a parabolic cylinder will be generated (refer to Figure 6) when a UV-laser with laser energy  $P_L$  scans over the resin surface in a straight line with a constant velocity  $V_s$ . Accordingly, the curing width and depth of the cured line's cross-section

will satisfy the parabolic equation:  $ay^2 + bz = c$ , where  $a = \frac{2}{W_0^2}$ ,  $b = \frac{1}{D_p}$ ,  $c = \ln \left\{ \sqrt{\frac{2}{\pi}} \frac{P_L}{W_0 V_s E_c} \right\}$ , and  $W_0$  is the

*Gaussian* half-width of the laser irradiance distribution (at the  $1/e^2$  point). Further deduction of the mathematical analysis can obtain the following important equation:

$$L_w = B \sqrt{\frac{C_d}{2D_p}} \quad (3.2)$$

where  $L_w$  is the line width and  $B \equiv 2W_0$ . This equation shows that the cured line width is proportional to the laser diameter, as well as the square root of the ratio between the curing depth and the resin penetration depth.

Similar to a laser beam, the focused spot of the UV-LED transmitted by the fiber optic light guide follows a *Gaussian* distribution. Consequently, liquid resin has similar curing behavior in our system. Hence, both equations (3.1) and (3.2) will be used in the modeling of our process.

#### 3.2. Experiment and Analysis

To verify the curing behavior of a focused UV-LED used in our system, experiments based on point curing were performed. As shown in Figure 7.(a), the point curing process is conducted as follows. We first turn on the UV-LED for a certain time. Accordingly, liquid resin will be cured on the tip of the light guide. The cured resin is in the shape of a bullet. For different exposure time, we measured the sizes of the cured bullets. Figure 7.b shows the relation between the curing depth and the input energy (measured by the curing time). The relation between  $C_d$  and  $\ln(E)$  matches Equation 3.1 quite well, which can be approximated by the following equation:

$$C_d = 1.0513 * \ln(T) + 1.2537 . \quad (3.3)$$

Based on the size measurement of the cured bullets, we can also approximate the relation between the curing width  $L_w$  and the curing depth  $C_d$  as shown in Equation 3.2 by the following equation:

$$L_w = 1.5016 \sqrt{C_d} . \quad (3.4)$$

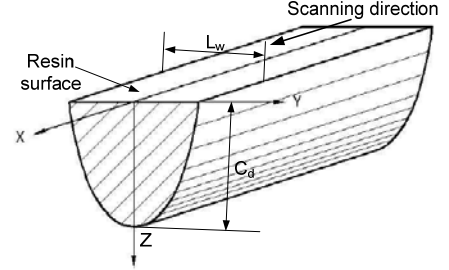


**Figure 6.** Parabolic cylinder of a cured line (Jacobs, 1992).

We further assume the curing behavior for point and line curing are identical. Therefore, Equations 3.3 and 3.4 would enable us to compute the curing depth and line width under different exposure time.

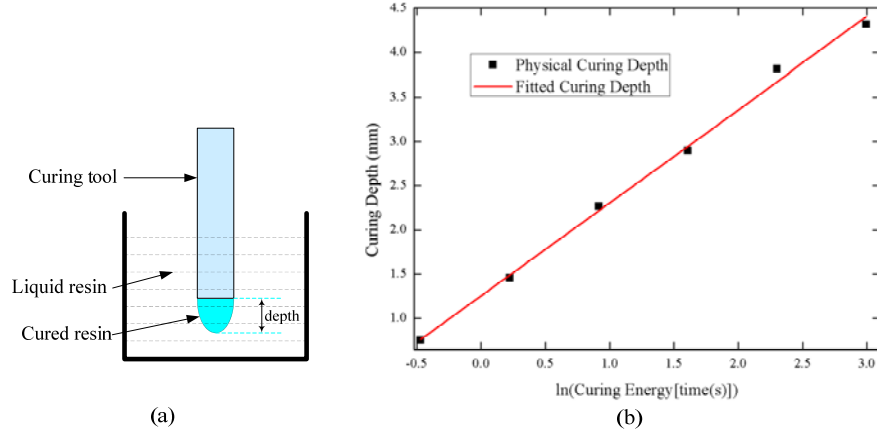


**Figure 7.** The curing depth versus the exposure energy for point curing.

## 4. ATTACHING OF POINT CURED RESIN

Since the newly cured resin in our process is always constrained between the curing tool and the base or the previously built part, the attaching forces on the two interfaces need to be modeled to ensure the building process to be successful.

### 4.1. Attaching Force Modeling

Suppose  $F_{Tool}$  is the attaching force between the cured resin and the tool; and  $F_{Base}$  is the attaching force between the cured resin and the base or the previously cured part. In order to separate the cured resin from the curing tool, we require:

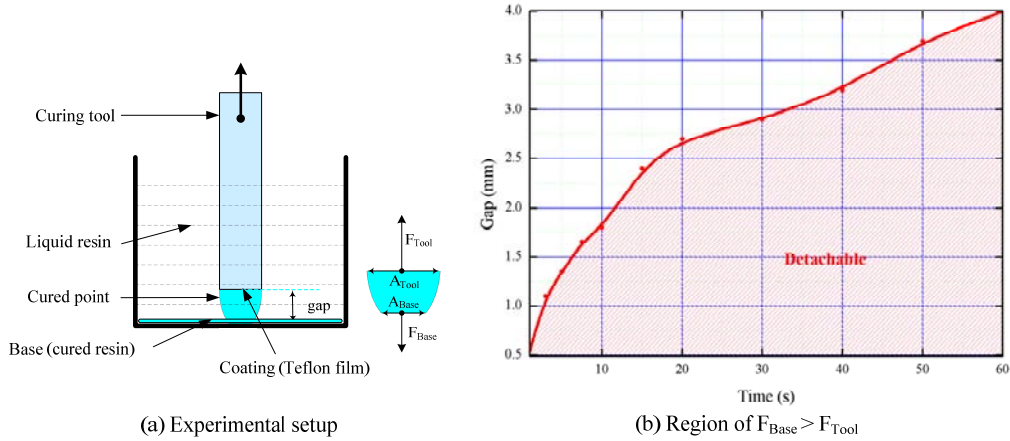
$$F_{Base} > F_{Tool} \quad (4.1)$$

An attaching force  $F$  can be determined by the following two factors:

- (1) The types of material that is in contact with the cured resin. Suppose a coefficient  $\alpha$  related to a given material is defined as the attaching force over a unit area. Hence, it is desired to have  $\alpha_{Tool}$  as small as possible while  $\alpha_{Base}$  as big as possible;
- (2) The attaching area  $A$ . As discussed in Section 3, suppose a bullet shape will be generated for the point curing. Hence, both  $A_{Tool}$  and  $A_{Base}$  can be estimated for a given curing time  $T$  and a gap  $d$  between the tool and the base. Note that the attaching area on the curing tool ( $A_{Tool}$ ) will always be bigger than that on the base or the previously built part ( $A_{Base}$ ). Further, for a smaller gap value  $d$ , the difference ( $A_{Tool} - A_{Base}$ ) will be smaller.

Hence, to ensure  $F_{Base} > F_{Tool}$ , we know:  $\alpha_{Base} \cdot A_{Base} > \alpha_{Tool} \cdot A_{Tool}$  or  $\frac{\alpha_{Base}}{\alpha_{Tool}} > \frac{A_{Tool}}{A_{Base}}$ . (4.2)

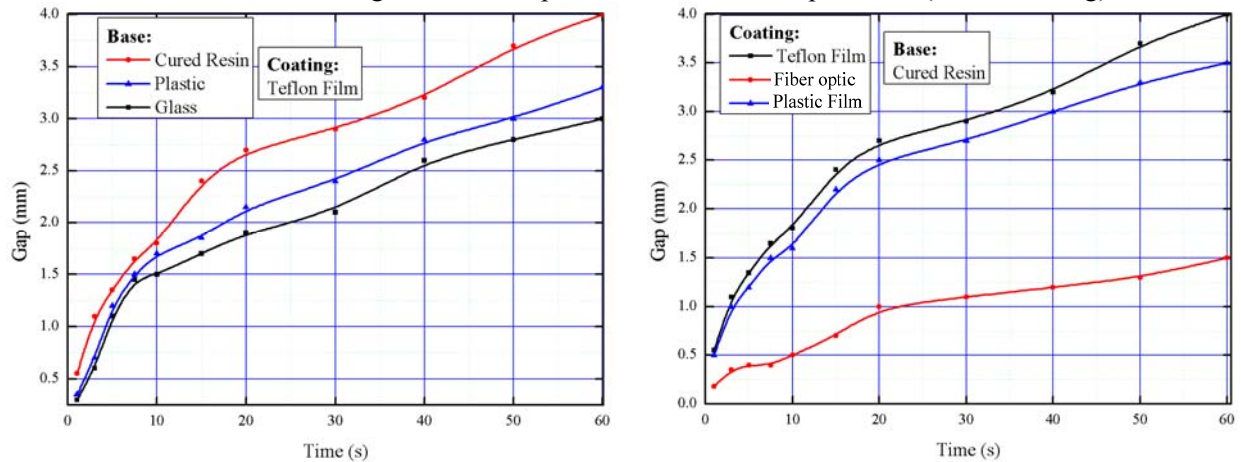
Our experimental setup for modeling the attaching forces of the point curing is shown in Figure 8.(a). We first position the curing tool to have a gap  $d$  to the bottom of the tank. After turning on the UV-LED for a certain time  $T_{Curing}$ , a portion of the resin will be cured and will attach to both the curing tool and the base. We then turned off the UV-LED and slowly move the light guide upwards. Consequently, (i) if  $F_{Base} > F_{Tool}$ , the cured resin will attach to the base; otherwise, (ii) the cured resin will attach to the curing tool. For different values of  $T_{Curing}$  and  $d$ , we record which side the cured resin will attach to, and accordingly generate a detachable region for the tested materials in the curing tool and the base. For example, a detachable region based on Teflon film and previously cured resin is shown in Figure 8.(b). The red points in the figure correspond to a critical state  $d_C$  where  $F_{Tool} \cong F_{Base}$ . The shaded portion under the curve denotes the detachable region, i.e., the settings in the region can ensure the newly cured resin attach to the previously cured resin instead of the curing tool. In addition, based on an identified critical state, the ratio  $\frac{\alpha_{Base}}{\alpha_{Tool}}$  for a curing time  $T_{Curing}$  can be estimated since  $\frac{A_{Tool}}{A_{Base}}$  related to  $d_C$  can be computed.



(a) Experimental setup (b) Region of  $F_{Base} > F_{Tool}$   
**Figure 8.** Attaching force study for the point curing.

#### 4.2. Experiments and Analysis

The detachable regions of various materials have been tested for the point curing. Figure 9.a shows, for a Teflon film as the tool material, a comparison between different base materials including plastics, glass and cured resin; Figure 9.b shows, for cured resin as the base material, a comparison between different tool materials including Teflon film, plastic film and fiber optic head (i.e. no coating).



(a) A comparison between different bases. (b) A comparison between different tool coatings.

**Figure 9.** Detachable regions of different materials for the point curing.

Based on the results, it can be observed that:

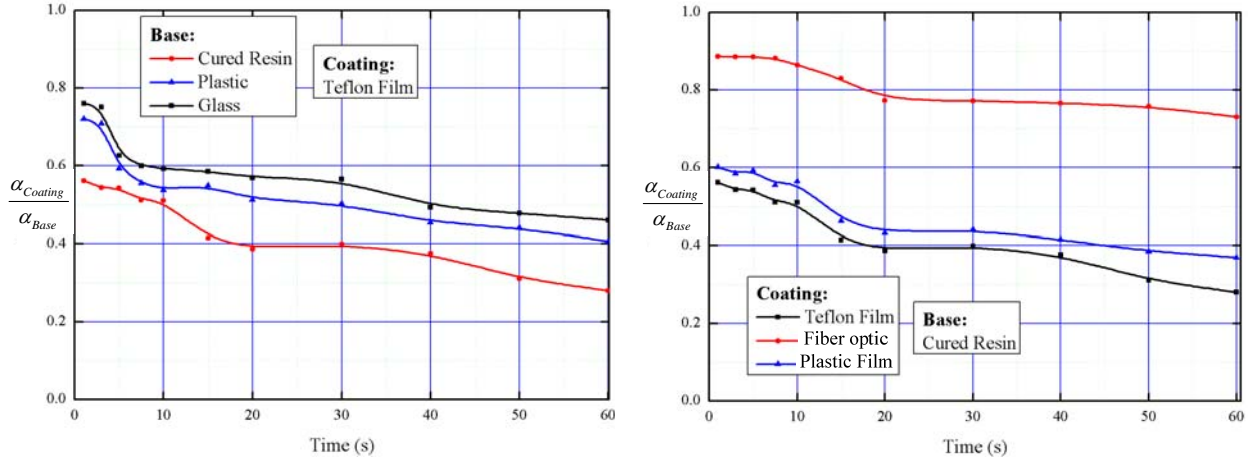
- (1) To ensure the building process to be successful, the exposure time should be increased if a bigger gap value is used;
- (2) For the same exposure time, using the cured resin and the Teflon film as the base and tool materials respectively can give us the largest safe region;
- (3) Since the fiber optic head has the smallest safe region, the CNC accumulation process will likely fail if no coating is applied on the tip of the tool.

The ratios  $\frac{\alpha_{Base}}{\alpha_{Tool}}$  related to different curing time ( $T_{Curing}$ ) are computed from  $\frac{A_{Tool}}{A_{Base}}$  based on the identified critical gaps, which are shown in Figure 10.

It can be observed from the figures that:

- (1) For all the materials, the attaching force coefficient ratio is decreasing as the curing time is increasing. That is, for a longer curing time, the attaching force on the coating is increasing faster than the attaching force on the base;

(2) Among all the coating and base materials, the pair of Teflon film and cured resin would give us the best performance. In addition, the average attaching force coefficient ratio between them is around 0.4.



(a) The comparison between different bases. (b) The comparison between different tool coatings. Figure 10. The relation between the attaching force coefficient ratio and curing time for point curing.

## 5. ATTACHING OF LINE CURED RESIN

Similar studies have been performed for the line curing, in which the curing tool is constantly moving in a direction that is orthogonal to the curing direction.

### 5.1. Attaching Force Modeling

During the line curing, the moving direction of the curing tool is different from its curing direction. Hence the attaching forces are mainly shearing forces as shown in Figure 11. We can use  $F_{Tool}$  as the shearing force between cured resin and the tool, and  $F_{Base}$  as the shearing force between cured resin and the base or the previously cured part. Hence, in order for the cured portion of the resin to successfully separate from the curing tool, it requires  $F_{Base} > F_{Tool}$ . Based on a similar procedure as discussed in

Section 4, a relation between the gap distance and the scanning velocity can be established (refer to Figures 12 and 13). The test results also show that using cured resin as the base and Teflon film as the tool coating would give us the best performance for line curing.

### 5.2. Experiments and Analysis

By moving the curing tool at a constant velocity  $V$ , portion of the resin between the tool and the base will be cured. The cured resin will attach to either the base if  $F_{Base} > F_{Tool}$ , or the tool if  $F_{Tool} > F_{Base}$ . Similar to the procedure used in Section 4.2, we identified the critical states  $d_C$  for various velocities, and accordingly built detachable regions for various materials. Figure 12.a shows, for a Teflon film as the tool material, a comparison between different base materials including plastics, glass and cured resin; Figure 12.b shows, for cured resin as the base material, a comparison between different coatings including Teflon film, plastic film and fiber optic head (i.e. no coating).

The relation between the attaching force coefficient ratio and the moving velocity in the line curing has also been established as shown in Figure 13. Compared to the point curing results as shown in Figure 10, it can be observed that:

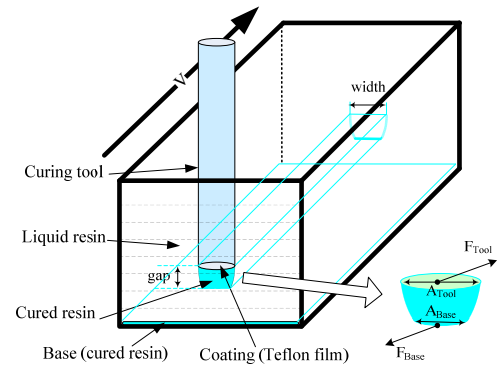
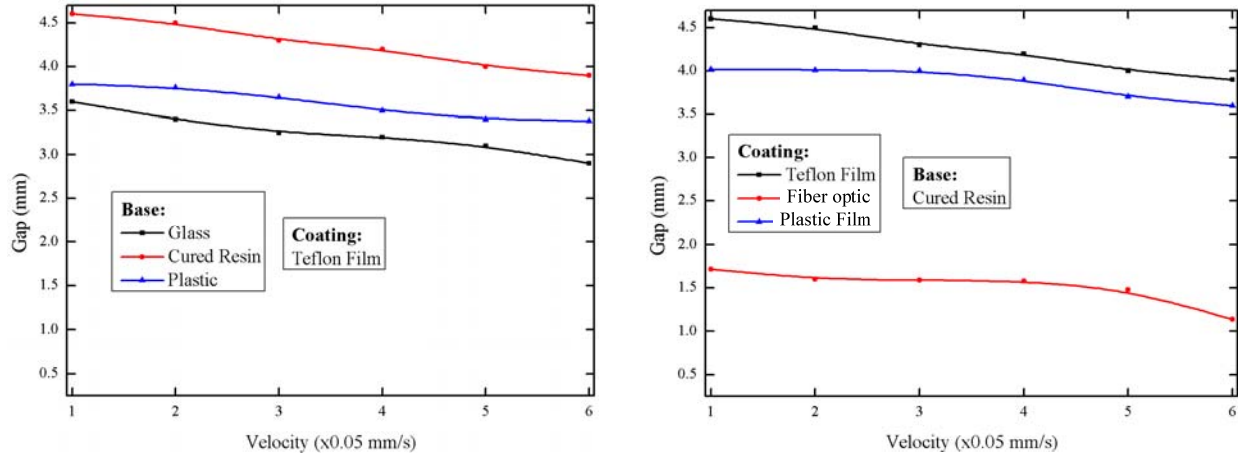


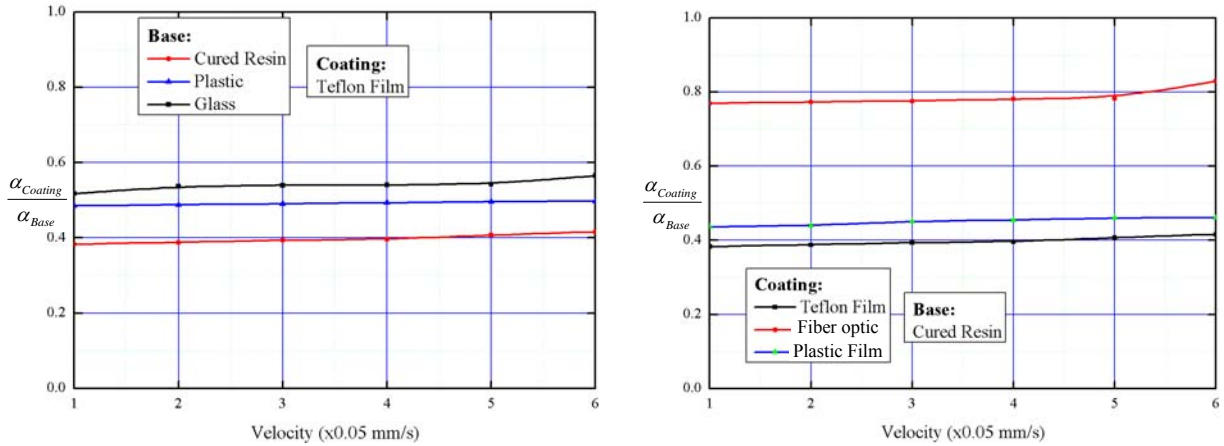
Figure 11. Attaching forces for the line curing.

- (1) The coefficient ratio for line curing is consistent to that of point curing. The relative sizes for the tested materials are:  $\alpha_{Cured\_Resin} > \alpha_{Plastic} > \alpha_{Glass} > \alpha_{Teflon\_Film}$  and  $\alpha_{Cured\_Resin} > \alpha_{Fiber\_Optic} > \alpha_{Plastic\_Film} > \alpha_{Teflon\_Film}$  for both point and line curing;
- (2) The force coefficient ratio for line curing is closer to a constant. In addition, such ratio values are close to the average values of  $\frac{\alpha_{Coating}}{\alpha_{Base}}$  in point curing.



(a) The comparison between different bases. (b) The comparison between different coatings.

**Figure 12.** The relation between the gap and scanning velocity for line curing.



(a) The comparison between different bases. (b) The comparison between different coatings.

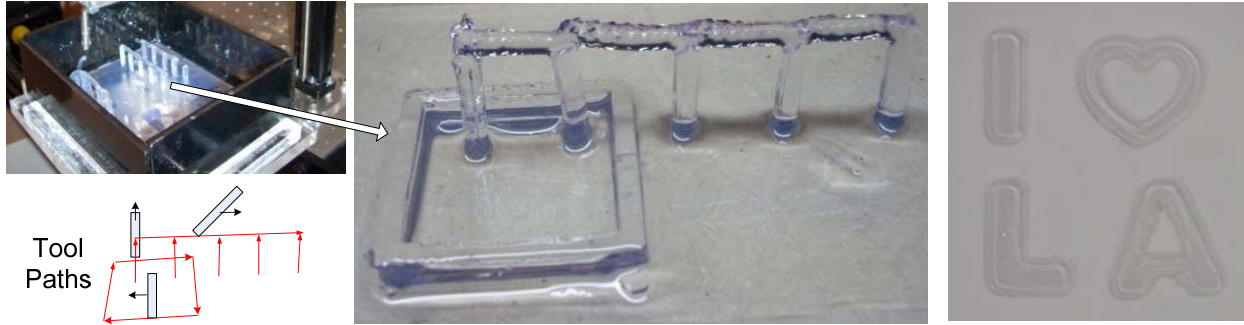
**Figure 13.** The relation between the force coefficient ratio and curing time for line curing.

## 6. CASE STUDY OF BUILDING VARIOUS GEOMETRIES

Case studies based on various 2D and 3D geometries have been performed. The experimental results have verified that the CNC accumulation process can build the given geometries, and achieve the material accumulation in different directions. In all the test cases, a Teflon film was applied as the coating on the fiber optic head.

### 6.1. 2D Curves

A simple square frame and a bridge structure were built to verify the capability of our process on building 2D curves. Both point and line curing as discussed in Sections 4 and 5 have been tested in the case (refer to Figure 14.a). A more complex 2D shape, a pattern of “I ♥ LA” as shown in Figure 14.b, was also tested. For an input CAD file that defines the pattern, we first used Mach3 CNC application to generate NC G-code. We then used the CNC accumulation controller to convert the generated G-code into control commands to build the part. Both test cases were built on the base of previously cured resin.



(a) A square frame and a bridge structure (b) "I love LA" character stroke  
**Figure 14.** Results of 2D curve study.

### 6.2. 2D Surfaces

A 2D planar surface as shown in Figure 15 was built to verify the capability of our process on building 2D surfaces. Based on the approach as shown in 2D curves, we first build two struts as supports. The 2D surface was then built by moving the curing tool along the tool path as shown in the figure. During the building process, the tool was kept at an angle to the surface such that the newly cured resin can be well bonded to the previously cured portion. As discussed in Sections 4 and 5, besides cured resin, other types of bases can also be used in our process. A test on different base materials was performed. In the test, an acrylic plastic plate was used, on which designed characters and decorating patterns were added (refer to Figure 16).

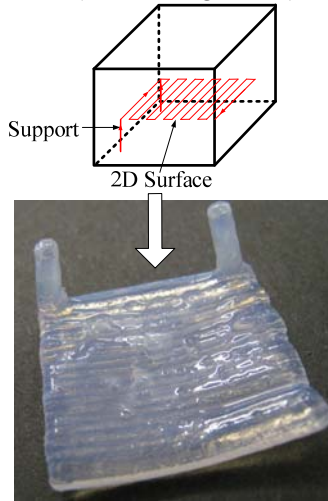


**Figure 15.** Test of a 2D planar surface.

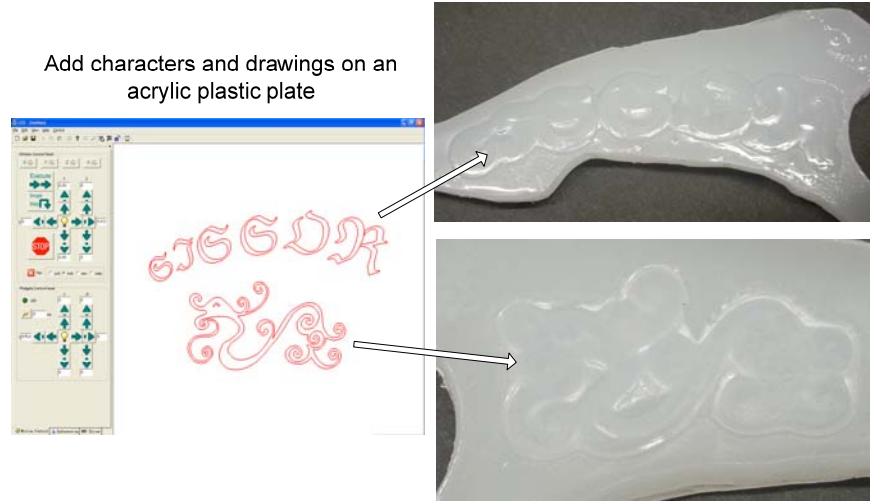


**Figure 16.** Results of 2D surface study: adding characters and dragon textures on a plastic plate.

### 6.3. 3D Curves

A half circle as shown in Figure 17 was built to verify the capability of our process on building 3D curves. In the building process, five struts were first added as supports. Since no layers are needed in the building process, the CNC accumulation process may improve the manufacturing efficiency for such geometries. In addition, in building the curve, we rotated the curing tool such that it has an angle that is close to the tangent direction of the curve. Hence, the built part can have an improved bonding strength along the curve.

A more sophisticated case as shown in Figure 18 was also performed. In the test, characters "USC FIGHT ON" were added on the inner surface of a plastic bowl. For the purpose, we first computed the G-Code for the 3D characters. We then computed the rotations of the bowl along Z axis, and the rotation of the curing tool along X axis for each character. Accordingly, the characters were successfully built. The bonding strength between the built characters and the plastic bowl has been tested to be satisfactory.

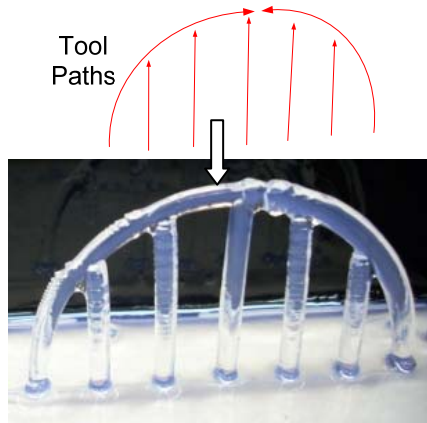


**Figure 17.** Test of a 3D curve.

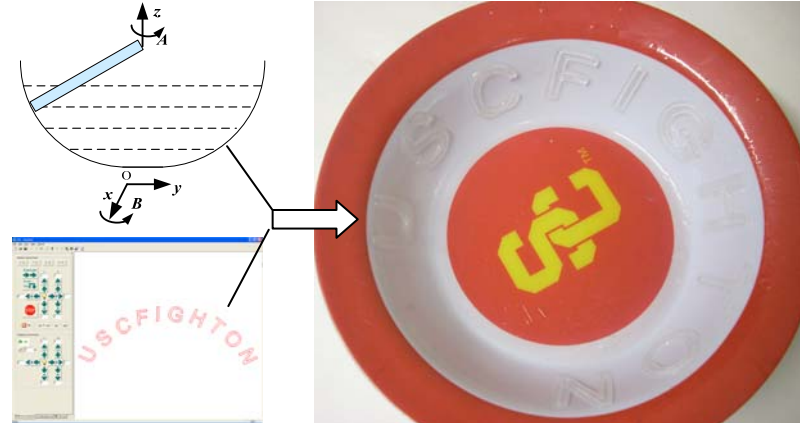


**Figure 18.** Test of spatial characters.

### 6.4. 3D Surfaces

A 3D cylindrical surface as shown in Figure 19 was built to verify the capability of our process on building 3D surfaces. Similar to the previous studies, supports were first built to facilitate the building process. The tool path and related building result are shown in Figure 19.a and b respectively. Note that a 2D and 3D surface built by the CNC accumulation process will still have anisotropic material property. However, based on design requirements, we can adjust such anisotropic behavior by planning different tool paths. For example, an alternative tool path for the built 3D surface is shown in Figure 19.c. In addition, the freedom on rotating the curing tool may also improve the material properties of built parts.

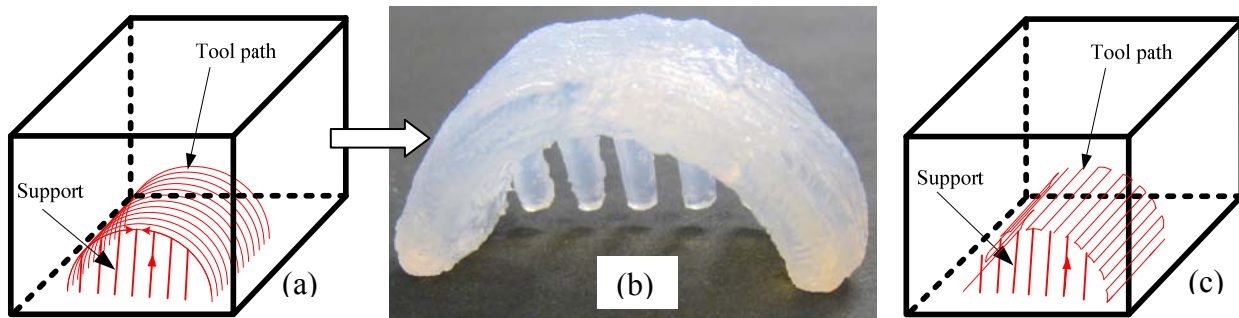


**Figure 19.** Test of a 3D cylindrical surface.

## 7. APPLICATIONS

### 7.1. Part Repairing and Modification

The AM processes such as laser engineered net shaping (Mudge and Wald, 2007), direct metal deposition (Liou, et al., 2007), and laser cladding (Kerschbaumer, et al., 2004) have been used in repairing metal parts and molds. However, there has yet to be an AM process that can repair plastic parts and molds. The developed CNC accumulation process can fill such a gap. A test case as shown in Figure 20 was performed to illustrate the capability of our process on adding features to a plastic part that was fabricated by other manufacturing processes. In the test, we first used the SLA process to build a CAD model (refer to Figure 20.a). Assuming a new feature is later identified and required to be added. Instead of throwing the part away and rebuilding the modified CAD model, we converted the new feature into related tool path (refer to Figure 20.b). We then positioned the SLA part on the tank. Based on the calibration of the part, the CNC accumulation process was used to build the new feature. Similar to the SLA process, the built model was fully cured after the building process. The modified part is shown in Figure 20.c. The bonding strength of the added feature is found to be satisfactory.

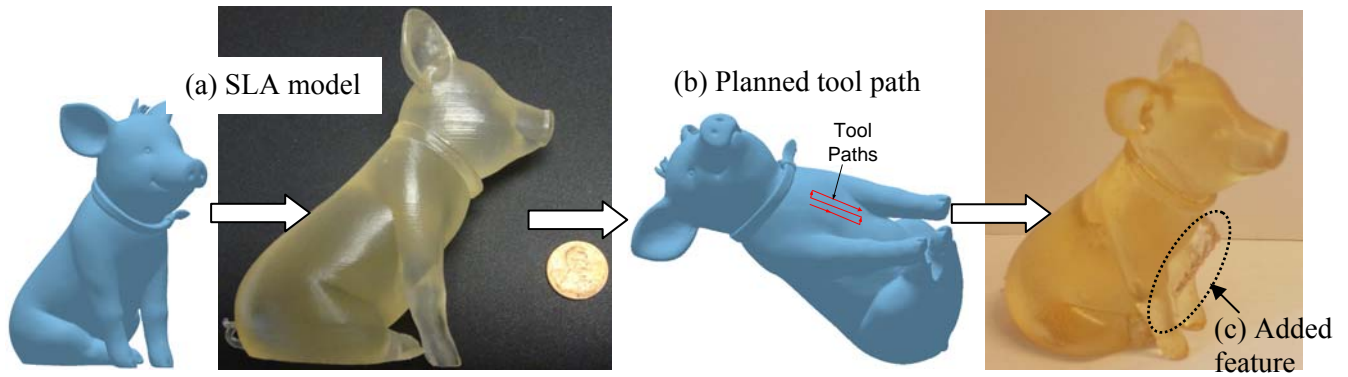


**Figure 20.** Test of part repairing and modification.

## 7.2. Building around Inserts

Current AM processes can only build parts with limited material options. In addition, a wide variety of components can be fabricated much more efficiently by other manufacturing processes. Hence, it is critical for future AM processes to address the requirement of building around inserts, i.e., the capability of integrating existing components that are made by other manufacturing processes in the AM building process. In the CNC accumulation process, a part can be built on various base materials from different building directions. Hence, the process can be beneficial for building around inserts. Four test cases are presented as follows to illustrate the capability of our process.

(1) **Adding a spring in a multi-functional scissor:** A scissor was first designed with two pieces that were laser-cut from an acrylic plastic plate. In the test, a spring needs to be added between the two plastic pieces such that the required motion of the scissor can be supported. In addition, it is desirable to use a standard metal spring since the spring will be repeatedly compressed and stretched. As shown in Figure 21, we used our system to successfully embed a metal spring with the two plastic pieces.

(2) **Adding a magnet bar in a multi-functional scissor:** In this test, a magnet bar needs to be added on the top surface of one plastic piece of the scissor such that the scissor can attract small metal parts. The tool path for embedding the magnet bar and the built scissor are shown in Figure 22. The embedded spring and magnet bar can successfully achieve the designed functionality.

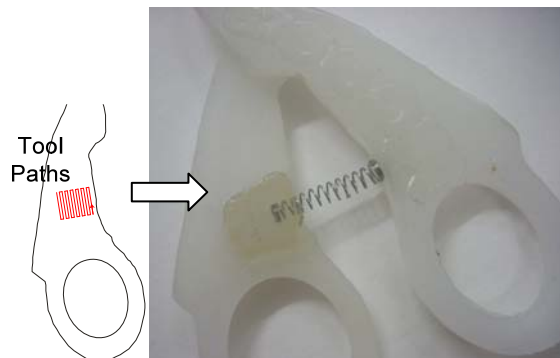


**Figure 21.** Test of adding a spring.

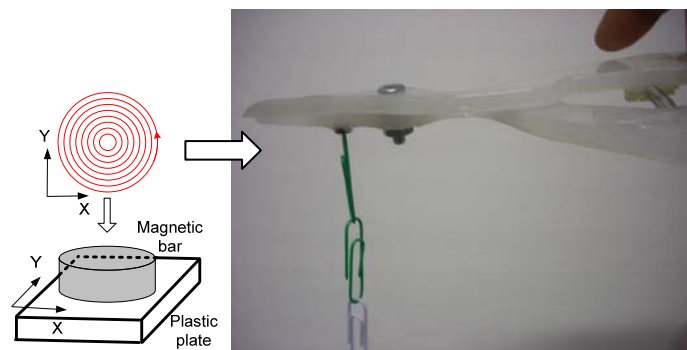


**Figure 22.** Test of adding a magnet bar.

(3) **Building a decoration part with optical fibers:** In the test, a decoration part in a star shape was designed, which has ten embedded optical fibers for transmitting light from a LED. The fixture of optical fibers is usually troublesome since the fibers generally have rather small sizes (e.g. a diameter of 0.25mm in our test). We first designed a fixture to position the optical fibers. Accordingly, a tool path was generated based on the designed shape. A plastic part with the embedded optical fibers was built, which is shown in Figure 23. Finally, one side of the optical fibers was connected to a controlled LED such that the built part with another side of the optical fibers can exhibit interesting lighting patterns.

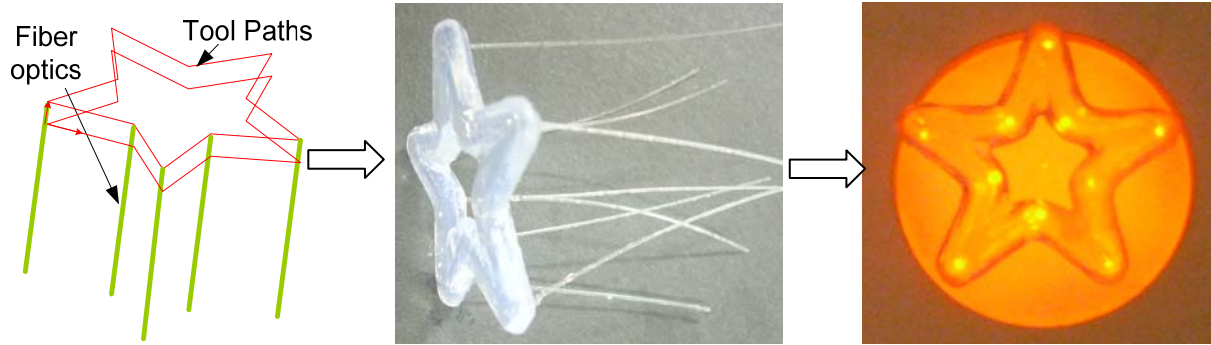


**Figure 23.** Test of building a decorating part with optical fibers.

(4) **Wrapping a resistor:** In the test, we demonstrate the capability of our process in wrapping existing electric components. Two resistors were used in the test, which are to be embedded in a built part. The tool path and related building result are shown in Figure 24.

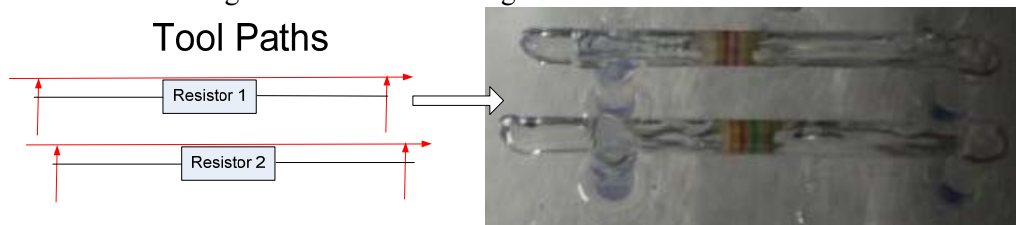


**Figure 24.** Test of wrapping resistors.

## 8. CONCLUSION

A layerless additive manufacturing process named CNC accumulation has been presented. In the process, multi-axis motion has been incorporated such that desired movements between the accumulation tool and the built part can be achieved. The curing mechanism of the process is similar to the SLA process. However, since the accumulation tool is merged under liquid resin, it is critical to model the attaching forces such that the building process can be ensured to be successful. Our study illustrates that a combination of Teflon film as the tool material and cured resin as the base material can present the biggest detachable regions for both point and line curing. Accordingly, a prototype system has been built, which integrated various hardware and software components. Based on such a system, case studies to verify the capability of the process on building various geometries have been performed. The effectiveness of the process for applications such as part repairing, part modification, and building around inserts has also been demonstrated.

There are plenty work that can be done to improve the developed process and related prototype system. Some current work we are investigating include: (1) developing curing tools with smaller size (e.g. 100-250  $\mu\text{m}$ ); (2) developing more sophisticated path planning algorithms which include the collision detection between the built part, the embedded part, and the curing tool; (3) exploring new applications that are enabled by our process.

## REFERENCES

1. Apro, K. (2009), *Secrets of 5-Axis Machining*, Industrial Press Inc., New York, NY.
2. Bourell, D., Leu, M., and Rosen, D. W. (2009), *NSF Workshop - Roadmap for Additive Manufacturing: Identifying the Future of Freeform Processing*, Washington, D.C., March 30-31, 2009.
3. Jacobs, F. P. (1992), *Rapid Prototyping and Manufacturing: Fundamentals of Stereolithography*, Society of Manufacturing Engineers, Dearborn, MI.
4. Kataria, A. and Rosen, D. W. (2001), "Building around inserts: method for fabricating complex devices in stereolithography". *Rapid Prototyping Journal*, Vol. 7, No. 5, pp. 253-261.

5. Kerschbaumer, M., Ernst, G., and O'Leary, P. (2004), "Tool Path Generation for 5-axis Laser Cladding", Proceedings of the LANE 2004, Vol. 2, pp. 831 – 842.
6. Liou, F., Slattery, K., Kinsella, M., Newkirk, J., Chou, H., and Landers, R. (2007), "Applications of a Hybrid Manufacturing Process for Fabrication of Metallic Structures", Rapid Prototyping Journal, Vol. 13, No. 4, pp. 236-244.
7. Mudge, R. P. and Wald, N. R. (2007), "Laser Engineered Net Shaping Advances Additive Manufacturing and Repair", Welding Journal, Vol. 86, No. 1, pp. 44 - 48.